Journal of Molecular Catalysis A: Chemical 347 (2011) 15–21

Contents lists available at ScienceDirect

Journal of Molecular Catalysis A: Chemical

journal homepage: www.elsevier.com/locate/molcata

Relationships between the efficiency of cyclohexane oxidation and the electrochemical parameters of the reaction solution

Alexander Pokutsa[a,*], Orest Fliunt[b], Yulia Kubaj[a], Tomasz Paczeŝniak[c], Pawel Blonarz[c], Ruslan Prystanskiy[a], Jacques Muzart[d], Roman Makitra[a], Andriy Zaborovskyi[a], Andrzej Sobkowiak[c]

[a] Department of Physical Chemistry of Combustible Fossils, Institute of Physical Organic Chemistry and Chemistry of Coal NAS of Ukraine, Naukova Str., 3A, Lviv 79053, Ukraine
[b] Lviv National University, Dragomaniv Str., 52, Lviv 79000, Ukraine
[c] Rzeszow University of Technology, P.O. Box 85, 35-959 Rzeszow, Poland
[d] CNRS – Université de Reims Champagne-Ardenne, Institut de Chimie Moléculaire de Reims, UMR 6229, UFR des Sciences Exactes et Naturelles, BP 1039, 51687 Reims Cedex 2, France

ARTICLE INFO

Article history:
Received 18 March 2011
Received in revised form 30 June 2011
Accepted 5 July 2011
Available online 14 July 2011

Keywords:
Cyclohexane oxidation
Vanadyl(IV)-acetylacetonate
Oxalic acid
Electrochemistry

ABSTRACT

Vanadyl(IV)-acetylacetonate-catalyzed oxidation of cyclohexane with H_2O_2, at 40 °C under air atmosphere, has been studied in the presence of small quantities of oxalic acid. The process efficiency is increased by this additive and depends on the nature of the solvent (MeCN ≥ MeOH > Me_2CO ≥ 2-PrOH > EtOH). The relationships between the results (conversion, yield) and the electrochemical characteristics of the reaction solution (relative permittivity, redox-potential) are highlighted and discussed.

1. Introduction

The oxidative functionalization of hydrocarbons is important from both practical and fundamental points of view. Cyclohexane oxidation is the basic process of the industrial-scale production of cyclohexanol and cyclohexanone [1,2] – these compounds being the precursors for Nylon-6 and Nylon-66 manufacturing [3,4]. The commercial homogeneous Co(II)-based process, which occurs at 160–180 °C, 1.3–1.5 MPa of air, leads to low (4–6%) conversions and moderate (75–80%) selectivities. Therefore, the elaboration of better protocols remains a challenge and their achievement can afford valuable information to carry out oxidative transformation of other hydrocarbons.

Previously, we disclosed that the efficiency of C_6H_{12} oxidation into $C_6H_{11}OH$, $C_6H_{10}O$, and $C_6H_{11}OOH$, at 40 °C and 0.1 MPa, using H_2O_2 as oxidant, $VO(acac)_2$ (**1**) as catalyst, and MeCN as the solvent is noticeably increased by addition of small amounts of glyoxal [5] and oxalic acid ($H_2C_2O_4$) (**2**) [6]. As appeared, the exchange of MeCN by EtOH was detrimental to this process [6]. Therefore, we assumed that this effect can be, among others, referred to the electrochemical parameters of the reaction solution (e.g., relative permittivity ε_r). Such an assumption is in agreement with literature data [7]. Nevertheless, in all previous reports, the kinetics of oxidation was studied exclusively in connection with ε_r values inherent to pure solvents. The possible modification of ε_r and the redox-potential of the reaction mixture by catalyst and additives has not been studied. Using low-frequency (10–10^5 Hz) dielectric spectroscopy (DS) [8,9] and cyclic voltammetry (CV) [10] techniques, we have tried to estimate the impact of the catalyst and additives on ε_r and the redox-potentials of the solutions, and to determine plausible relationships between these parameters and the reaction efficiency. These two methods have emerged as the most powerful noninvasive electrochemical tools to investigate the mechanism of oxidation processes [11,12]. The solvents for the oxidation, CV, and DS experiments have been chosen according to their various relative permittivity values as well as to their ability to be inert under the experimental conditions and to dissolve reagents and products. MeCN, MeOH, Me_2CO, 2-PrOH, and EtOH agree with these requirements.

2. Experimental

2.1. Chemicals

The commercial aqueous solutions of hydrogen peroxide (35 wt.%, Fluka) have been concentrated by vacuum distillation at 45 °C/10 mm Hg to 70 wt.% (caution: risk of explosion. All glassware has to be thoroughly rinsed by distilled water to remove traces

* Corresponding author. Tel.: +380 32 263 51 74; fax: +380 32 263 51 74.
E-mail address: apokutsa@ukr.net (A. Pokutsa).

1381-1169/$ – see front matter © 2011 Elsevier B.V. All rights reserved.
doi:10.1016/j.molcata.2011.07.003

of any heavy metals). As the commercially available vanadyl(IV)-acetylacetonate (Aldrich) is of ca. 95% purity only, the crude $VO(acac)_2$ was dissolved in MeCN to give a saturated solution, which was then filtrated through a micro-porous paper filter. The filtrate was evaporated at 40 °C under reduced pressure, and the resulting solid was dried under vacuum at 20 °C for 48 h, leading to dark-green tiny (0.5–1 mm) crystals which were used in the oxidation experiments. Cyclohexane, acetonitrile, methanol, ethanol, 2-propanol, acetone, triphenylphosphane, and tetra-n-butyl ammonium perchlorate (all from Aldrich) were used as purchased.

2.2. Experimental installation and oxidation reactions

The catalytic experiments were carried out in 25-mL round-bottom glass flasks equipped with reflux condenser and magnetic stirrer. In a typical experiment, 3.36 g (40 mmol, 1.8 mol L^{-1}) of cyclohexane were dissolved in 15 mL of MeCN containing 0.0032 g (0.012 mmol, 5×10^{-4} mol L^{-1}) $VO(acac)_2$ and 0.038 g (0.3 mmol, 0.014 mol L^{-1}) oxalic acid. The mixture was heated at 40 °C for 5 min before 1.34 g (40 mmol, 1.8 mol L^{-1}) of H_2O_2 were added. This moment corresponds to the beginning of the oxidation reaction. Usually, the reaction has been carried out for 5 h under atmospheric pressure.

The values of relative permittivities (ε_r) of the reaction solution have been obtained by dielectric spectroscopy (DS) measurements [8]. The dielectric response of any medium is characterized by the spectral shape of the real (in-phase) $\varepsilon_1(\omega)$ and imaginary (quadrature) $\varepsilon_2(\omega)$ components of the dielectric complex constant $\varepsilon^*(\omega) = \varepsilon_1(\omega) - j\varepsilon_2(\omega)$ or by the corresponding complex capacitance $C^*(\omega) = C_1(\omega) - jC_2(\omega)$, where j is the imaginary unit and ω is the angular frequency; $C_1(\omega)$ and $C_2(\omega)$ are the real and imaginary components of the complex capacitance, respectively. Complex capacity and complex ε_r are connected via the constant factor S/d by the equation: $\varepsilon_r^* = C * /d(\varepsilon_0 S)$, where S is the area of contacts of the plane capacitor, m^2; d the thickness of polarization region, m; ε_0 the relative permittivity of vacuum (8.85×10^{-12} F m^{-1}) [8,9]. In some cases the use of complex capacity instead of complex dielectric constant have some advantages, particularly, when electrode or double layer polarization effects dominate on the spectra. Dielectric spectra in the frequency range of 10–10^5 Hz have been measured by transducing the complex capacity into sinusoidal voltage on the basis of operational amplifier [8]. This method eliminates the influence of stray capacitors of connecting cables. Sinusoidal voltage 100 mV rms was applied to the measuring cell. Phase shifts were measured using a digital phase-meter. Calibration of the equipment using etalon elements permits to exclude the constant bias errors. A 10-mL glass vial equipped with two parallel stainless steel electrodes (1 mm × 10 mm × 20 mm) with fixed 2 mm inter-electrode distance has been used as the measuring cell. Usually, the total volume of reaction mixture was 8 mL. All experiments have been conducted at room temperature and atmospheric pressure. After each measurement, the electrodes have been copiously rinsed by distilled water and then thoroughly dried.

Cyclic voltammetry (CV) measurements of the redox potential of the reaction mixtures have been carried out at room temperature using an EG & G Princeton Applied Research potentiostat/galvanostat model 273A. The experiments were conducted in a 15-mL glass electrochemical cell containing 10 mL (total volume) of reagents. In order to provide proper electrolytic conditions, the voltammograms have been taken in the presence of tetra-n-butyl ammonium perchlorate (0.1 mol L^{-1}). The working electrode was a Bioanalytical Systems glassy-carbon (area, 0.09 cm^2) inlay, the auxiliary electrode a platinum wire, and the reference electrode an Ag/AgCl/Cl^- wire, in an aqueous tetramethylammonium chloride solution that was adjusted to give a potential of 0.00 V vs SCE. The later was contained in a Pyrex tube with a cracked soft-glass tip, which was placed inside a Luggin capillary [10]. Before each CV measurement, argon was bubbled through the reaction solution for at least 30 min to remove dissolved oxygen. After the experiment, the deposits, contaminating the active edge of the working electrode, have been removed by polishing it with a Gamma Micropolish II Alumina (0.05 μm, Buehler) paste, followed by copiously rinsing with distilled water and then thorough drying. A microportion of H_2O_2 (usually 0.3 mmol) has been injected into the mixture of reactants under vigorous stirring; that moment was considered as the starting point for current–voltage depended function measurements.

2.3. Analysis of the reaction products

The reaction mixture was sampled at regular intervals. The content of products in the samples was analyzed using a GLC Hewlett–Packard 5890, series II (flame-ionization detector, capillary column 30 m × 0.25 mm, immobile phase HP-Innowax) as well as a LKhM-80 one (flame-ionization detector, packed column 3 m × 3 mm, immobile phase OV-17 on Chromaton N-AW). Prior to the analyses, a 2-butylbenzene solution in ethanol was added as internal standard to the withdrawn sample. The identification of the oxidation products was performed by comparison with the retention times of commercial cyclohexanol and cyclohexanone. Subsequently, both the conversion and the selectivity towards the obtained products were determined by the common calculation procedure. The quantification of the oxygenated products was performed using a multi-points calibration line plotted using references of $C_6H_{11}OH$ and $C_6H_{10}O$. In order to determine the proper content of cyclohexanol, cyclohexanone, and cyclohexyl hydroperoxide, each probe was analyzed twice by GC – before and after the addition of triphenylphosphane. In the presence of PPh_3, the $C_6H_{11}OOH$ is rapidly and quantitatively transformed into $C_6H_{11}OH$; then the true content of cyclohexylhydroperoxide can be calculated as the difference between the $C_6H_{10}O$ and $C_6H_{11}OH$ concentration before and after the triphenylphosphane addition [13]. Titration of probes of the reaction mixture by an aqueous 0.10 mol L^{-1} solution of $Na_2S_2O_3$ in presence of KI allows to determine the amount of H_2O_2 which has been consumed.

3. Results and discussion

Oxidation of C_6H_{12} has been carried out using from 1 to 10 equivalents of H_2O_2, a catalytic amount of $VO(acac)_2$ (**1**), and various quantities of oxalic acid (**2**). The main results are collected in Table 1 (for all experiments, the process selectivity calculated on the sum of aimed products was 97–99%). Accordingly to the results shown in Table 1, the addition of **2** led to a noticeable improvement of the process. For example, in MeCN, the presence of **2** increases both the conversion and TON (compare entries 1 and 2), the optimal amount of **2** being between 0.011 and 0.022 mol L^{-1} (Fig. 1). Exceeding this amount drops the alkane conversion.

Studies on the positive influence of pyrazine-2-carboxylic [14,15], sulfuric or oxalic acid [16] as a co-catalyst on the V_2O_5 and $NaVO_3$-catalyzed oxidations of alkanes led us to suspect that oxalic acid acts also with the reduced form of catalyst (V^{4+}), this plausibly leading to the coordination of its monoanion to the metal cation. Diminution of the oxidation efficiency caused by an excess of **2** can be attributed to the acceleration of the heterolytic cleavage of H_2O_2 at very low pH values [17] (pH equal −2 was reached in the case of amounts of **2** higher than 0.010 mol L^{-1}). The alkane conversion increases to 30% in the presence of **2** when the C_6H_{12} concentration was decreased to 0.18 mol L^{-1} (entry 4). According to these data, the most appropriate medium for C_6H_{12} oxidation is

Table 1
Oxidation of C_6H_{12} in five solvents in the presence of $VO(acac)_2$ and oxalic acid.[a]

Entry	c (**2**), mol L^{-1}	Solvent	Conversion, %	Selectivity (product spread), %[b]			TON, mol mol^{-1} (**1**)	ΔH_2O_2[c], %	E_c[d], mol%
				$C_6H_{11}OH$	$C_6H_{10}O$	$C_6H_{11}OOH$			
1	–	MeCN	1.6	33	62	5	33	48	3.3
2	0.014	MeCN	5.3	48	7	45	169	96	5.5
3	0.14	MeCN	5.2	47	10	43	173	80	6.5
4[e]	0.014	MeCN	30	22	44	34	944	34	8.8
5	–	MeOH	1.6	65	20	15	52	21	7.6
6	0.014	MeOH	3.6	83	17	<1	120	66	5.5
7	–	2-PrOH	1.1	43	29	28	35	27	4.1
8	0.014	2-PrOH	2.2	52	31	17	72	43	5.1
9	–	EtOH	0.1	11	61	28	3	2	5
10	0.014	EtOH	0.7	33	38	29	22	10	7
11	–	Me_2CO	0.2	57	8	35	6	78	0.3
12	0.014	Me_2CO	2.5	17	14	69	85	84	3.0

[a] $c(C_6H_{12}) = c(H_2O_2) = 1.8$ mol L^{-1}, c (**1**) $= 5 \times 10^{-4}$ mol L^{-1}, total reaction volume 22 mL, 40 °C, 5 h.
[b] So far the process selectivity was ca. 99% the %yield of each products was equal it selectivity and the total yield (in mol L^{-1}) can be estimated as conversion of $C_6H_{12} \times c(C_6H_{12})/100$.
[c] Amount of consumed H_2O_2 (i.e., conversion of H_2O_2).
[d] Effectiveness (E_c) of the H_2O_2 consumption: $E_c = c(C_6H_{12}{}^{converted})/\{c(C_6H_{12}{}^{initial}) \times \Delta H_2O_2\}$.
[e] $c(C_6H_{12}) = 0.18$ mol L^{-1}, $c(H_2O_2) = 1.8$ mol L^{-1}, c (**1**) $= 5 \times 10^{-5}$ mol L^{-1}, total reaction volume 22 mL, 40 °C, 5 h.

acetonitrile whereas the worst one is EtOH. The average difference in the conversion of cyclohexane and TON between these two solvents was more than 10 times. The solvent-dependent oxidation efficiency, including the effectiveness of H_2O_2 consumption (E_c, Table 1) was in the following order: MeCN ≥ MeOH > Me_2CO ≥ 2-PrOH > EtOH, regardless of the presence or absence of the additive.

The additive, besides its influence on the hydrocarbon conversion and yield, also modify the proportion of the products. For example, the $C_6H_{11}OH/C_6H_{10}O/C_6H_{11}OOH$ ratio in MeCN varies from 6.6/12.4/1.0 (entry 1) in the absence of an additive to 1.0/0.2/1.0 when **2** is added (entry 2). In contrast to acetonitrile, 2-propanol, ethanol, and acetone, the amount of $C_6H_{11}OOH$ formed in MeOH was very low (Table 1, entry 6). The relative yield of $C_6H_{11}OH$ and $C_6H_{10}O$ can also be modified by the nature of the solvent and the presence of **2** (Table 1). Compared to EtOH, the better results in MeOH are a consequence of the well-known free-radicals termination by the ethanol molecules [18]. Such feature of the oxidation in EtOH can refer to its noticeably lower value of ε_r (24.5) and its higher donor number (32.0) in comparison to those of MeOH (32.7 and 19.0, respectively) [19]. That trait in conjunction with the ability of alcohols to form strong intermolecular hydrogen bonds (as in water which is another powerful quencher of the free-radical species) leads to the better solvation of free-valent species (see part devoted of the DS studies below), hence lowers the generation of exclusively radical-dependent products ($C_6H_{11}OOH$, Table 1).

It is known that the process rate is linked by some manner to the solvent's relative permittivity, ε_r [7,12,19]. Nevertheless, a possibly existing relationship between ε_r of the reaction mixture and the main process characteristics has not been examined yet. According to the data of Table 1, both conversion and yield depend on solvent, catalyst, and additive. It was logical to assume that catalyst and additive can modify ε_r of the reaction medium, and thus affect the whole process effectiveness. In order to elucidate this assumption, low-frequency dielectric spectra of the reaction mixtures used have been measured and four typical ones are presented at Fig. 2. The values of ε_r have been calculated from the curved lines (the real part of spectra) whereas the electric conductivity of the reaction medium can be obtained from the straight lines (imaginary part of spectra). According to Fig. 2, the dependences of $C_1(\omega)$ vs frequency show a strong dispersion towards the low frequencies region, which is related to electrode polarization. In the high-frequency region, the dispersion of the real part of capacity was not observed; this allows to calculate the relative permittivity constant of the liquid using plane capacitor formula. The imaginary part of capacity $C_2(\omega)$ decreases with increasing frequency accordingly to the $1/\omega$ law. Such relationships give an opportunity to characterize the solutions by the values of non-dispersive conductivities. Given the data of Table 1, the oxidation in methanol and 2-propanol occurs in yields which are only slightly lower than

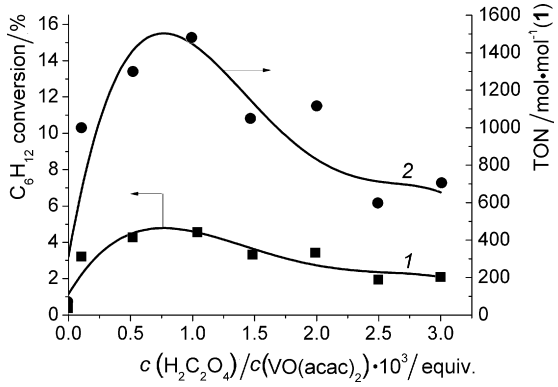

Fig. 1. Cyclohexane conversion (1) and process TON (2) depending on the oxalic acid content. Oxidation conditions: $c(C_6H_{12}) = 1.8$ mol L^{-1}, $c(VO(acac)_2) = 5 \times 10^{-4}$ mol L^{-1}, $c(H_2O_2) = 1.8$ mol L^{-1}, in MeCN at 40 °C, 5 h.

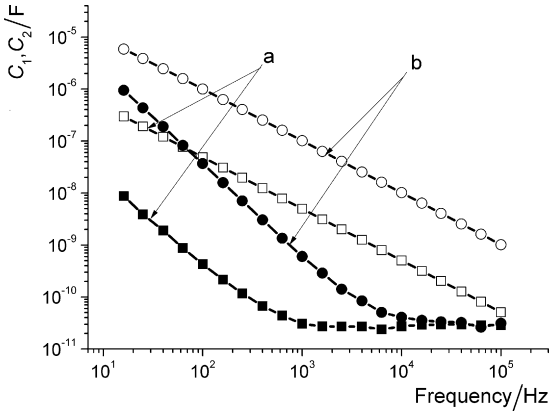

Fig. 2. Low-frequency dielectric spectra of **1** (a) and **1** + **2** (b) solutions in MeCN at 20 °C. Solid and open symbols correspond to the real (C_1) and imaginary (C_2) parts of capacity. Concentration of catalyst and activator was the same as in the oxidation experiments (see Table 1, footnotes).

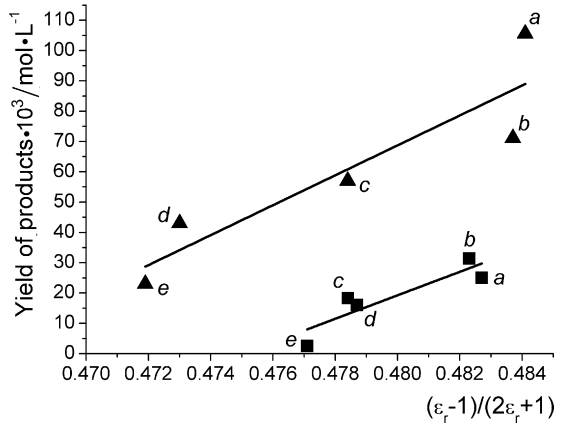

Fig. 3. The total yield of products vs Kirkwood parameter in dependence of components presented in the started reaction mixture: squares – in presence of **1**, triangles – in presence of **1** + **2**. (a) MeCN, (b) MeOH, (c) Me_2CO, (d) 2-PrOH, (e) EtOH. Concentration of catalyst and activator was the same as in the oxidation experiments.

in MeCN, whereas the process ceased almost completely in EtOH. The effect has been asserted to the values of the Kirkwood parameter $(\varepsilon_r - 1)/(2\varepsilon_r + 1)$ of the reaction medium, which is linked to the oxidation products yields by the linear law shown in Fig. 3. The addition of **2** caused the slight increase in ε_r of the solutions of **1** in MeCN (from 42.9 to 47.3) and MeOH (from 41.6 to 45.8). Contrary to these solvents, adding of **2** into EtOH or 2-PrOH decreases the relative permittivity from 32.1 to 26.3 and 34.7 to 27.3, respectively, whereas in acetone this value remains almost constant and is equal to 34.2 (when **2** is present in the reaction mixture the difference in relative permittivity between MeOH and EtOH solutions grows from about 30% for the **1**-based process up to 74% for the **1** + **2** one). The linearity displayed by these dependencies, regardless of the absence or presence of **2** (Fig. 3), can be referred to the predominance of the electrostatic solute/solvent interaction (non-specific solvation) over the electron-pair donor/electron-pair acceptor (EPD/EPA) interaction (specific solvation). In general, their ratios are considered to about 4:1 [20]. The activated complexes formed in the absence and presence of **2** have rather similar dipole moments because of the same slope of the lines in Fig. 3 [18]. Some deviation from linearity, particularly observable when **2** is present in the reaction mixture (Fig. 3), can be a result of specific (non-electrostatic) solvation of the reactive species [18]. The observation that the oxidation is more efficient in MeCN than in MeOH and is extremely slow in EtOH, can also be due to other characteristics of the solvents used: (*i*) their donor numbers (DN) which are equal to 14.1 for MeCN, 19.0 for MeOH, and 32.0 for EtOH, and (*ii*) their dipole moments which are actually proportional to ε_r and dropped from μ = 3.53 D (MeCN) to 2.87 D (MeOH) and 1.66 D (EtOH) [20]. It is found that the efficiency of C_6H_{12} oxidation is only slightly lower in MeOH as compared to MeCN (Fig. 3) which are characterized by close numbers of both DN and dipole moment, but it is dramatically diminished in EtOH which possesses the highest DN and the lowest dipole moment. According to the literature [19,20], solvents with a relatively small DN (MeCN, MeOH) solvate metal ions rather weakly particularly those in their higher oxidation state. Hence, in such solvents, the M^{n+1} can be easily reduced to M^{n+}, making M^{n+1} a strong oxidizing agent. The experimental data reported in Fig. 3 support these assumptions and provide a good reason to subject the yield to ε_r of the reaction solution. Nevertheless, the dependencies of C_6H_{12} oxidation may be related, besides the parameters of non-specific solvation, also to DN. Furthermore, the contribution of the solvent's electrophilicity (proportional Lewis acidity), basicity (proportional Lewis basicity), and the intermolecular hydrogen bond donor/acceptor capability (specific solvation's parameters) cannot be completely removed from our consideration.

Despite the observation that relative alteration of the ε_r value caused by addition of **2** was quite negligible (1.1–1.2 times), this addition sets off a conspicuous increase (in 2.5–7 times) of the conversion and yields in all solvents (Table 1 and Fig. 3). This finding can be related to the properties of particular cations and anions studied in solution. The matter is that the solvation of $VO(acac)_2$ and $H_2C_2O_4$ is favored by the relative permittivity of the solvent and the charge on the solute species in accordance to the Born model [21] (albeit rather in the first approximation due to the data [22]). On the other hand, in agreement with the HSAB concept [23], hard VO^{2+} cations coordinate better to the hard (and smaller) $HC_2O_4^-$ anion than to the soft (and bulky) $acac^-$ anion. The dissociation of $VO(acac)_2$ is facilitated in polar solvents (MeCN, Me_2CO, MeOH). For solvents possessing a high relative permittivity and a relatively small DN (MeCN, MeOH), we assume that the metal cation (VO^{2+}) interacts preferably with $HC_2O_4^-$ than with $acac^-$ [20]. Hence, the rate of ligands rearrangement should be determined by the medium polarity as postulated in a number of reports [24–26]. The putative adduct of the first-stage interaction between H_2O_2 and $VO(HC_2O_4)_2$ ($[VO(HC_2O_4)_2 \ldots H_2O_2]$) possesses a higher density of the positive charge than $[VO(acac)_2 \ldots H_2O_2]$ (see the results of calculation below). Hence, this primary adduct would be better solvated by polar solvents in accordance to the general concepts: if the charge density of an activated complex increases, the corresponding process rate would be enhanced with increasing solvent polarity because of the lowering of the activation energy of the reaction [18,27]. Given the quantum-chemical calculations (PM6) [28], a noticeable benefit in energy was developed when the two acac ligands of $VO(acac)_2$ were substituted by two HC_2O_4 (ΔH_f° decreased from $-239.25\ kcal\ mol^{-1}$ for $VO(acac)_2$ to $-442.26\ kcal\ mol^{-1}$ for $VO(HC_2O_4)_2$) [29]. Simultaneously, such a ligands exchange lowers the charge density on the metal from +1.08 eV to +1.22 eV [29]. The easier coordination of H_2O_2 by $VO(HC_2O_4)_2$ can lead to both quick generation of hydroxyl radicals and formation of alternative (to the $HO^\bullet$) high-valent vanadium-oxo species active and selective in hydrocarbon oxidation [6,13,14]. In the last case H_2O_2 is consumed much more sufficiently (Table 1) as compared to the homolytic way of its decomposition (more details of this assumption are reviewed in the CV part below). Therefore, the acceleration of the oxidation process in the presence of **2** would be a result of two factors – the medium polarity and the modification of the electron density of the metallocomplex cation caused by the $acac^-/HC_2O_4^-$ ligand exchange. The exclusive assignment of the effect of the acid to the transformation of the vanadate anion into oligomeric oxovanadates as postulated in [16] looks questionable. Indeed, the reduction of the oligomeric vanadium(V) ion into vanadium(IV) by hydrogen peroxide as it was assumed in [16] is rather difficult because of the high oxidizing and low reducing abilities of H_2O_2. In contrast, a reasonable explanation is plausible if we take into consideration the particular reducing properties of oxalic acid (see also the CV part below).

Changes in the charge of these ionic solutes in the reaction mixture occurring in the course of the redox process affect the value of electric current flows between the electrodes when the applied potential is varied. Application of the CV technique for the generated current registration can supply valuable information about the concentration of the redox species and their modification in the course of the chemical process. Therefore, some important conclusions concerning the process kinetics and the reactions mechanism can be made. In Figs. 4–6 and Figs. S1–S3 the voltammograms of **1** and **1** + **2** in MeCN are presented which have been taken before and after the H_2O_2 addition. The forward anodic scan of the initial light-blue solution of $VO(acac)_2$ (Fig. 4, curve 1) displayed the oxidation peak at 0.98 V, which is coupled with the reduction one appearing at 0.92 V in the reverse scan. The second reduction peak emerges at −1.84 V and is irreversible (Fig. 4, curve 1). During the second

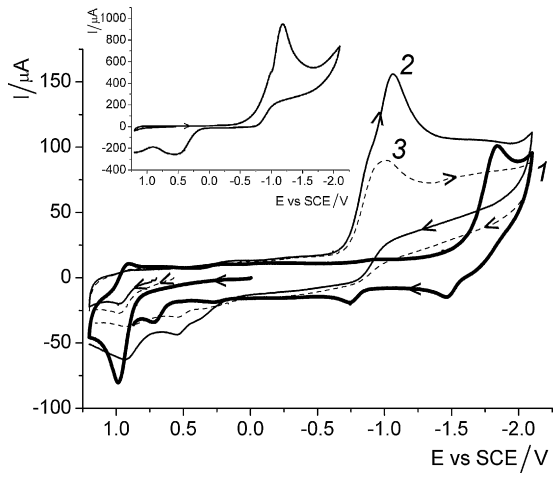

Fig. 4. CV diagram of the 1×10^{-3} mol L^{-1} $VO(acac)_2$ solution in MeCN (1) and the same solution drawn, respectively, at 2 (2) and 3 (3) min after of 0.3 mmol H_2O_2 injection (anodic scan). Inset: CV of 1×10^{-3} mol L^{-1} $VO(acac)_2$ solution preliminary saturated by O_2.

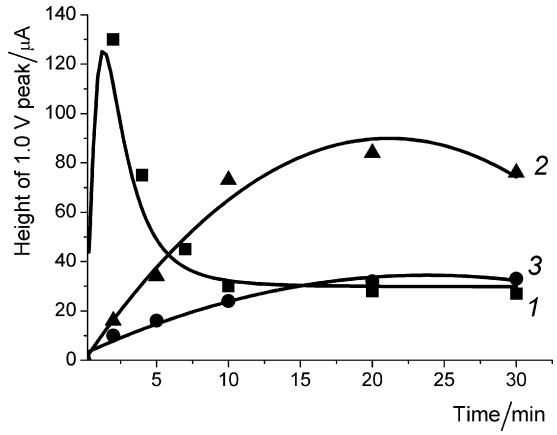

Fig. 5. The kinetic of the −1.0 V peak height changes on CV of the **1** + **2** solution after addition of 0.3 mmol H_2O_2 in dependence of the oxalic acid content: squares – 0 (1), triangles – 1.0 (2), circles – 5×10^{-3} mol L^{-1} (3) of **2**; $c(VO(acac)_2) = 1 \times 10^{-3}$ mol L^{-1}.

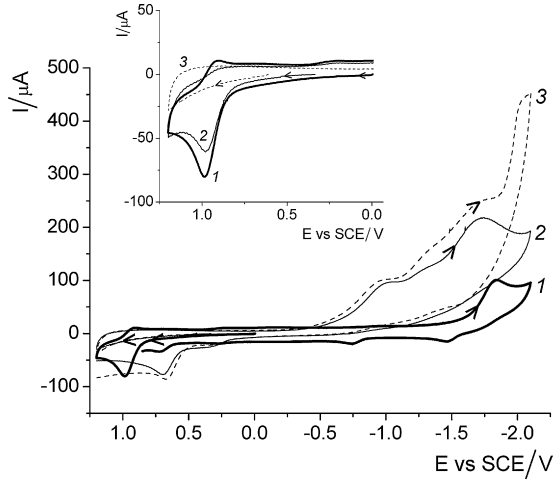

Fig. 6. CV diagram of the 1×10^{-3} mol L^{-1} solution of $VO(acac)_2$ in MeCN (1), 1×10^{-3} mol L^{-1} $VO(acac)_2 + 5 \times 10^{-3}$ mol L^{-1} oxalic acid (2), and the last solution drawn after 5 min of 0.3 mmol H_2O_2 injection (3), (anodic scan). Inset: CV of the V^{IV} peak shape vs content of oxalic acid: 1 – 0, 2 – 0.2, 3 – 1.0×10^{-3} mol L^{-1} concentration of **2**.

cycle of this initial positive scan four oxidation peaks are appeared at −1.45, −0.74, 0.30, and 0.72 V, respectively (Fig. 4, curve 1). The forward catodic scan of the same solution (Fig. S1, curve 1) resulted in one irreversible reduction peak at −1.84 V. Four oxidation peaks appear at the same places (−1.45, −0.74, 0.30, and 0.72 V) in anodic scanning when the second cycle of this catodic scan was drawing. Simultaneously, a reduction peak at 0.66 V, reversible to the one appeared at 0.72 V, becomes visible in the second cycle of this negative scan too. Due to the data reported for similar systems by Kitamura and Reichel [30–32], the distinct reversible couple at 0.98 and 0.92 V (Fig. 4 and Fig. 1S, curve 1) exhibits without doubt the $V^{IV} \leftrightarrows V^{V}$ process, while the couple at 0.72 and 0.66 V (Fig. S1, curve 1) can be referred to the $V^{IV} \leftrightarrows V^{III}$ one. A corroboration that the last redox reaction can take place is that the ions in their lower oxidation state (V^{III}) are oxidized (and respectively reduced) at a less positive potential [31] (a discussion of the last assumption proceeds below). These facts also point out that the redox reactions studied involve in fact a one electron exchange. The peaks at −1.84 V and 0.30 V presented in the voltammograms 1 result from both anodic (Fig. 4) and catodic (Fig. S1) scans and can be attributed to the redox reaction of the acac ligands, respectively (Fig. S2, inset) [31,33].

The addition of H_2O_2 into the initial solution of $VO(acac)_2$ causes a dramatic and rapid increase of the peak situated near −1.0 V (Fig. 4 and Fig. S1, curves 2). Nevertheless, in 5 min this peak is reduced (Fig. 4, curves 2 and 3) back to the value found before the H_2O_2 addition with almost the same rate as it was growing (Fig. 5, curve 1). Saturation of the $VO(acac)_2$ solution by O_2 resulted in an extremely high peak appearance which was observed at about −1.0 V (Fig. 4, inset). Therefore, the discussed peak with a maximum at −1.0 V (Fig. 4 and Fig. S1, curves 2) can be assigned to the dioxygen released in the course of the fast H_2O_2 decomposition catalyzed by $VO(acac)_2$. Furthermore, the last mentioned reaction leads to a quick transformation of the parental catalyst ions (V^{IV}) into their oxidized form (V^{V}) that substantiates the noteworthy diminishing of the oxidation peak at 0.98 V (Fig. 4, curve *2*). The surplus wide oxidation peak appeared in the voltammogram near 0.5 V as well as the broad reduced peak at about −1.7 V (Fig. 4, curve 2) are inherent to H_2O_2 (Fig. S2, curve 1).

The profile of CV for the **1** + **2** mixture sufficiently differs from the one depicting solely $VO(acac)_2$ (compare curves 1 and 2 in Fig. 6 and Fig. S3). First of all, the peak was assigned to the oxidation of V^{IV} (0.98 V), steadily diminished when the $H_2C_2O_4$ concentration increases from 0 via 0.2 to 1.0 mmol–L^{-1} (Fig. 6, inset). Continuation of the second anodic (Fig. 6) and catodic (Fig. S3) scans results in some broad heel extended from 0.3 to 1.2 V (curves 2) which eventually hides the peak at 1.0 V. The height of this last peak is lower almost twice as much compared to the one presented in curves 1. It means that vanadium ions in oxidation state IV are not attended in the mixture any more if the amount of oxalic acid added exceeds one equivalent of $VO(acac)_2$. Secondly, the peak previously attributed to the oxidation of V^{III} (0.72 V), in the presence of oxalic acid noticeably increased (compare curve 1 and 2, Fig. 6). The last marked changes as well as the fact of almost complete disappearance of the oxidation peak at −0.98 V in the presence of oxalic acid (Fig. 6, curve *2*) confirm the possibility of the chemical reduction of initial V^{IV} species towards V^{III} by **2**. Interestingly, the addition of H_2O_2 into the solution of **1** + **2** causes a rather negligible changes (compared to the oxalic acid-free process) in the peak attributed to released O_2 (near −1.0 V) as well as to the one at −1.7 V assigned to free H_2O_2. The kinetics of the −1.0 V peak height changes (Fig. 5) depicts clear relationships between the presence of oxalic acid and the concentration of O_2 in the solution (i.e., rate of the H_2O_2 cleavage). In the absence of **2**, the sharp enhancing of the dioxygen content in the solution followed by its abrupt decrease was observed almost instantly after the H_2O_2 injection (Fig. 5, curve 1). Contrary to the previous case, the presence of about

1.0 mmol L^{-1} oxalic acid leads to the much more gentle slope of the curve characterizing the kinetics of O_2 (curve 2). Increasing the concentration of **2** up to 5 mmol L^{-1} causes a further flattening of the curvature of the respective line (compare curve 2 and 3).

The revealed differences in the behavior of the electrochemical processes in the absence and presence of **2** and H_2O_2 help to get a proper reply concerning the mechanism of the selective cyclohexane oxidation enhanced by oxalic acid. Based on the experimental data we are now able to conclude that: (*i*) so far the acid-free process is characterized by the rapid O_2 release, one can assume that it can be the result of quick homo- and heterolytic decomposition of the peroxide. The homolysis of H_2O_2 via the Haber–Weiss mechanism resulted in free-radicals (mainly $HO^{\bullet}$). The extremely active (although non-selective) hydroxyl-radicals react with any surrounded molecule, that is substrate, solvent and H_2O_2. Therefore, in the case of radical-based oxidation, the percentage of productive consumption of hydrogen peroxide should be lower compared to the non-radical (enzyme-like) mechanism. The last mechanism is presumably favored under **2** assistance [6] since its presence in the $VO(acac)_2$-based reaction improves the process, i.e., yield, TON, and E_c (Table 1). Due to the kinetics, electrochemical, and quantum-chemical calculation [29] data, the activating ability of **2** can be consisted in the efficient chelation of the transition-metal cations by **2**, this leading to withdraw the charge density from the metal core of the catalyst. The consequences could be an easier access of peroxide molecules to the catalyst, and thus an increase of the rate of homolytic decomposition of H_2O_2 is accelerated [29]. On the other hand, the coordination of **2** to the catalyst cation can simultaneously facilitate the formation of the high-valent vanadium-oxo species as it is proposed in [6,34]; (2) the reducing properties of oxalic acid prompt the reactions like $M^{n+1} + \mathbf{2} \rightarrow M^{n+} + CO_2$ [35], particularly if the redox potential of metal cations (V^V/V^{IV} = 1.0 V) is lower than that of H_2O_2 (1.77 V) [36]. The electrochemical data by preferable reduction of V^{IV} over its oxidation in the presence of **2** are in good agreement with the above-mentioned quantum-chemical calculations and also match well with previously published results [6]. In summary, one can conclude that the redox properties of

$$V^{IV}O + H_2C_2O_4 \rightarrow V^{III}(OH) + CO_2 + {}^{\bullet}CO_2H \quad (1)$$

$$V^{IV}O + H_2O_2 + 1/2\,O_2 \rightarrow V^{V}O_2 + HO^{\ominus} + HO^{\bullet} \quad (2)$$

$$V^{V}O_2 + {}^{\bullet}CO_2H + HO^{\ominus} \rightarrow V^{IV}O + H_2O + CO_2 + 1/2\,O_2 \quad (3)$$

$$VO(acac)_2 + H_2C_2O_4 \rightarrow [VO(HC_2O_4)_2] + acacH \quad (4)$$

$$VO(acac)_2 + H_2C_2O_4 + e^{\ominus} \rightarrow \{[(acac)_2V\cdots O\cdots H_2C_2O_4]^{\ominus}\}^{\neq} \rightarrow [(acac)V(OH)(HC_2O_4)] + acac^{\ominus} \quad (5)$$

$$[(acac)V(OH)(HC_2O_4)] + H_2C_2O_4 \rightarrow [V(OH)(HC_2O_4)_2] + acacH \quad (6)$$

$$[V(OH)(HC_2O_4)_2] - e^{\ominus} \rightarrow [VO(HC_2O_4)_2] + H_2C_2O_4 \quad (7)$$

$$[VO(HC_2O_4)_2] - e^{\ominus} \rightarrow \{[(HC_2O_4)V\cdots O\cdots C_2O_3H]^{\oplus}\}^{\neq} \rightarrow [VO_2(HC_2O_4)] + CO + {}^{\bullet}CO_2H \quad (8)$$

Scheme 1.

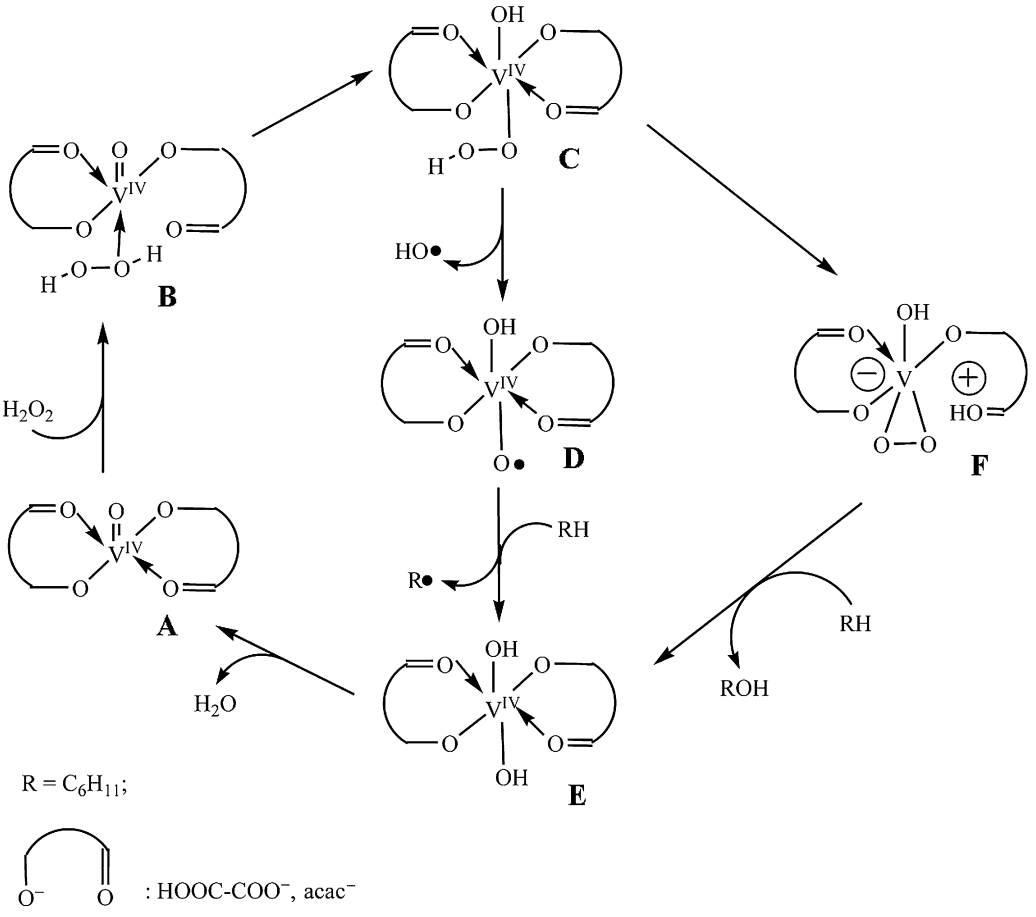

Scheme 2.

the catalyst can be modulated by the activator used. This fact is imprinted in the electrochemical characteristics of the reaction mixture which are affected by the presence of oxalic acid and have a distinct impact on the whole catalytic oxidation process.

The key putative steps accompanying both the stoichiometrical and electrochemical reactions of reduction and oxidation of $VO(acac)_2$ in the presence of oxalic acid [35] are presented in Scheme 1. Reaction 1 by which free $^{\bullet}CO_2H$ radicals are formed, as well as the electrochemicalReaction (8) can be considered as those which determined the rate of the process. Reaction (2) is responsible among others for the quick growing of the O_2-peak on the CV diagram (Fig. 4, curve 2) after the addition of H_2O_2 into the $VO(acac)_2$ solution. The formyl-oxo radicals are the reducing agent for the oxidized form of metal cation (Reaction (3)) (in reactions (5) and (8) the intermediated species are marked by $^{\neq}$). Vanadyl(IV)oxalate formed in situ from vanadyl(IV)acetylacetonate and oxalic acid (reaction (4)) can lead to the oxo- (**D**) and peroxo- (**F**) species due to the putative Scheme 2 [6]. Such species are presumably responsible for the acceleration of the radical and non-radical steps of the oxidation process in presence of oxalic acid. In accordance to the Scheme 2, the process would occur via a radical pathway represented by $\mathbf{A} \rightarrow \mathbf{B} \rightarrow \mathbf{C} \rightarrow \mathbf{D} \rightarrow \mathbf{E} \rightarrow \mathbf{A}$ [14,34,37], and a non-radical one illustrated by $\mathbf{A} \rightarrow \mathbf{B} \rightarrow \mathbf{C} \rightarrow \mathbf{F} \rightarrow \mathbf{E} \rightarrow \mathbf{A}$. The $\mathbf{F} \rightarrow \mathbf{E}$ transformation would involve interactions of cyclohexane at the second coordination sphere of **F**. Under our oxidation conditions, cyclohexanol, cyclohexanone and cyclohexyl hydroperoxide are generated simultaneously, with different rates, from the beginning of the oxidation process. The clear co-catalytic nature of **2** in the process (besides of it reduction properties) can be displayed by the next simple calculation. As follows from the Table 1 (entry 2) the total amount of products formed from C_6H_{12} can be estimated as: $TON \times c(\mathbf{1}) = 169 \times 0.0005 = 0.0845\ mol\ L^{-1}$, whereas the initial amount of **2** was noticeably lower ($0.014\ mol\ L^{-1}$). The co-catalytic function of oxalic acid is also depicted in Scheme 2.

4. Conclusions

The acceleration effect induced by the addition of small amounts of oxalic acid on the rate of the cyclohexane oxidation as well as the relationships between the electrochemical properties of the reaction mixture (relative permittivity and redox potential) from one side and the oxidation process characteristics from the other one have been highlighted and explicated. The yield of products and their ratio depend on the nature of the solvent and the additive. The practical interest of the above study lies in the ability to forecast the oxidizing system reactivity, thanks to the determination of the electrochemical properties of the reaction mixtures.

Acknowledgements

Authors are indebted to Prof. J. Kowalski and Dr. O. Pereviznyk for helpful discussions as well as to Mrs. D. Maksym for her assistance in the manuscript preparation. This work was supported by NATO CLG No. 982510.

Appendix A. Supplementary data

Supplementary data associated with this article can be found, in the online version, at doi:10.1016/j.molcata.2011.07.003.

References

[1] Y. Ishii, S. Sakaguchi, T. Iwahama, Adv. Synth. Catal. 343 (2001) 393–427.
[2] U.F. Kragten, H.A.C. Baur: EP Pat. 659,726 (1995);
U.F. Kragten, H.A.C. Baur, Chem. Abstr. 123 (1995) P86595r.
[3] A.P. Tomilov, S.K. Smirnov, Adiponitrile and Hexamethylenediamine , Khimiya, Moskwa, 1974 (in Russian).
[4] M. Eissen, J.O. Metzger, E. Schmidt, U. Schneidewind, Angew. Chem. 114 (2002) 402–425;
M. Eissen, J.O. Metzger, E. Schmidt, U. Schneidewind, Angew. Chem. Int. Ed. 41 (2002) 414–436.
[5] A. Pokutsa, J. Le Bras, J. Muzart, Kinet. Catal. 48 (2007) 26–31.
[6] A. Pokutsa, Yu. Kubaj, A. Zaborovskyi, D. Maksym, J. Muzart, A. Sobkowiak, Appl. Catal. A: Gen. 390 (2010) 190–194.
[7] R.G. Makitra, R.E. Prystanskii, R.B. Sheparovich, Russ. J. Phys. Chem. 78 (2004) 522–525.
[8] E. Barsoukov, J.R. Macdonald, Impedance Spectroscopy Theory, Experiment, and Applications , second ed., Wiley, Hoboken, 2005.
[9] A.J. Bard, L.R. Faulkner, Electrochemical Methods. Fundamentals and Applications , second ed., Wiley, New York, 2001.
[10] D.T. Sawyer, A. Sobkowiak, J.R. Roberts Jr., Electrochemistry for Chemists , Wiley, New York, 1995.
[11] G.R. Facer, D.A. Notterman, L.L. Sohn, Appl. Phys. Lett. 78 (2001) 996–999.
[12] C.R. Keese, J. Wegener, S.R. Walker, I. Giaever, PNAS 101 (2004) 1554–1559.
[13] G.B. Shul'pin, Y.N. Kozlov, L.S. Shul'pina, P.V. Petrovskiy, Appl. Organomet. Chem. 24 (2010) 464–472.
[14] G. Shulpin, Yu. Kozlov, G. Nizova, G. Suss-Fink, S. Stanislas, A. Kitaygorodskiy, V. Kulikova, J. Chem. Soc. Perkin Trans. 2 (2001) 1351–1371.
[15] R. Khaliullin, A. Bell, M. Head-Gordon, J. Phys. Chem. B 109 (2005) 17984–17992.
[16] L.S. Shul'pina, M.V. Kirillova, A.J.L. Pombeiro, G.B. Shul'pin, Tetrahedron 65 (2009) 2424–2429.
[17] C. Walling, Acc. Chem. Res. 8 (1975) 125–131.
[18] N. Emanuel, G. Zaikov, Z. Maizus, Oxidation of Organic Compounds. Medium Effects in Radical Reactions , Pergamon Press, Oxford, 1984.
[19] C. Reichardt, Solvents and Solvent Effects in Organic Chemistry , third ed., Wiley-VCH, Weinheim, 2003.
[20] K. Izutsu, Electrochemistry in Nonaqueous Solutions , Wiley-VCH, Weinheim, 2002.
[21] M. Born, Z. Phys. 1 (1920) 45–48.
[22] J.E. Gordon, The Organic Chemistry of Electrolyte Solutions , Wiley, New York, 1975.
[23] R.G. Pearson, in: N.B. Chapman, J. Shorter (Eds.), Advances in Linear Free Energy Relationships, Plenum Press, London/New York, 1972 (Chapter 6).
[24] A.J. Parker, Chem. Rev. 69 (1969) 1–32.
[25] N. Greenwood, A. Earnshaw, Chemistry of the Elements , Pergamon, Oxford, 1984.
[26] A. Cotton, G. Wilkinson, C. Murillo, M. Bochmann, Advanced Inorganic Chemistry , sixth ed., Wiley, New York, 1999.
[27] A.A. Frost, R.G. Pearson, Kinetics and Mechanism , Wiley, New York, 1961.
[28] J.J.P. Stewart, J. Mol. Model. 13 (2007) 1173–1213.
[29] A. Pokutsa, Yu. Kubaj, A. Zaborovskyi, R. Prystanskyi, J. Muzart, R. Makitra, T. Mysakovych, D. Maksym, A. Sobkowiak, Unpublished results, prepared for submission to Kinet. Catal.
[30] M. Kitamura, K. Yamashita, H. Imai, Bull. Chem. Soc. Jpn. 49 (1976) 97–100.
[31] M.-A. Nawi, T.S. Reichel, Inorg. Chem. 20 (1981) 1974–1978.
[32] M. Kitamura, K. Yamashita, H. Imai, Chem. Lett. (1975) 1071–1974.
[33] M.-A. Nawi, T.S. Reichel, Inorg. Chem. 21 (1982) 2268–2271.
[34] M.V. Kirillova, M.L. Kuznetsov, V.B. Romakh, L.S. Shul'pina, J.J.R. Fraústo da Silva, A.J.L. Pombeiro, G.B. Shul'pin, J. Catal. 267 (2009) 140–157.
[35] V. Srinivasan, J. Roček, J. Am. Chem. Soc. 96 (1974) 127–133.
[36] R.A. Sheldon, J.K. Kochi, Oxid. Combust. Rev. 5 (1973) 135–242.
[37] G.B. Shul'pin, Mini Rev. Org. Chem. 6 (2009) 95–104.